On the detectability of roller bearing damage by frequency analysis

Y-T Su, PhD and **Y-T Sheen,** MSc
Department of Mechanical Engineering, National Sun Yat-Sen University, Kaohsiung, Taiwan

This study investigates the detectability of roller bearing damage by the frequency analysis of bearing vibrations. The magnitude characteristics of peaks in the vibration spectra are analysed. It is shown that the frequency information of vibration spectra for undamaged roller bearings can be the same as that for damaged ones. However, the magnitude information of vibration spectra for undamaged roller bearings is different from that for damaged ones. Thus, to detect the initial fault of roller bearing reliably, both the frequency information and magnitude information of vibration spectra have to be used.

1 INTRODUCTION

Frequency analysis is one of the most commonly applied methods for bearing initial fault detection. When there is a damage on the bearing surface, the damaged spot will periodically contact the matching surface and induce a periodic pulse train which will have an impact on the bearing system. This impact will cause the vibration spectra of a damaged bearing to have a pattern of equal frequency spacing distribution (EFSD) (**1**). The EFSD pattern shows that there are peaks (defined as main peaks) equally spaced with an interval related to the frequency (defined as the defect frequency) of the impact train. Around each peak, there are side bands equally spaced with an interval related to the periodicities of the transmission path (**2**) and loading zone (**1**). Because the impact pulse is short, the EFSD pattern will appear up to a high-frequency band. Thus, the high-frequency resonance technique (**3**) becomes an effective tool in disclosing the existence of the EFSD pattern with little influence of other noises. It is assumed that the examined bearing is damaged when the EFSD pattern is detected.

However, it is found that when running under large preload (**4**) or at high speed (**5**) the vibration spectra of undamaged roller bearings (such as a cylindrical roller bearing or tapered roller bearing) may also have the EFSD pattern. The frequency information of the EFSD pattern for undamaged bearings is the same as that for damaged bearings. The studies showed that the occurrence of the EFSD pattern for undamaged bearings is induced by the surface irregularities of bearing components. When a roller rotates, the surface irregularities of the roller and races cause the oil-film thickness to change and induce a dynamic force acting at the roller and the races. This dynamic force excites the bearing assembly and causes the bearing to vibrate. The frequency characteristic of this dynamic force is the same as that of periodic pulse trains due to defect. Thus, the vibrations induced by surface irregularities have a similar signature to that induced by surface damage. The stiffness of an oil film or the magnitude of a dynamic force may be enhanced by increasing the running speed or axial loading. Thus, under these running conditions, the vibration induced by surface irregularities dominates the other sources of vibrations and has a clear EFSD pattern. This result demonstrates that the existence of the EFSD pattern does not necessarily indicate damage of roller bearings. Accordingly, the reliability of frequency analysis for roller bearing condition monitoring is questionable.

This study will show that the magnitude information of demodulated spectra for undamaged roller bearings is very different from that for damaged ones. Thus, to obtain a reliable condition monitoring for roller bearings, both the frequency information and the magnitude information of demodulated spectra at a high-frequency band should be examined. In the following, the magnitude characteristics of demodulated spectra for both undamaged and damaged roller bearings are first examined. Then several experiments are demonstrated to verify the analytical study.

The MS was received on 28 July 1992 and was accepted for publication on 9 December 1992.

2 MAGNITUDE CHARACTERISTICS OF VIBRATION SPECTRA FOR UNDAMAGED ROLLER BEARINGS

Consider a roller bearing with surface irregularities (from the manufacturing process) on its components. Assume that the rollers are spaced equally along the circumference of races. When the bearing rotates, due to excitation of surface irregularities, a dynamic force is induced at the matching surface between the roller and each race (**4–6**). If a sensor is located in housing at a fixed site, the frequency characteristics of measured vibrations, corresponding to the mth mode vibrations of the bearing assembly, can be described by (**4**)

$$
\begin{aligned}
X^s_m(\omega) = \Bigg[\sum_{p=1}^{2} \sum_{q=1}^{2} \Bigg\{ & n_0 \sum_{i_1} \sum_{i_2} \sum_{i_4} Y_{\mathrm{T}1p}(i_1\omega_{yp}) K'_{\mathrm{T}1q} \\
& \times (i_2\omega_{k'q}) A_{\mathrm{T}1m}(i_4\omega_a) \\
& \times \delta(\omega - i_1\omega_{yp} - i_2\omega_{k'q} - i_4\omega_a)\delta_{\mathrm{T}} \\
& \times (\text{integer} \times n_0 - i_1 - i_2 - i_4) \Bigg\} \\
+ \sum_{n=1}^{n_0} \sum_{p=1}^{2} \Bigg\{ & \sum_{i_1} \sum_{i_2} \sum_{i_4} Y_{\mathrm{T}np}(i_1\omega_{yp}) \\
& \times K'_{\mathrm{T}n3}(i_2\omega_{k'3}) A_{\mathrm{T}nm}(i_4\omega_a) \\
& \times \delta(\omega - i_1\omega_{yp} - i_2\omega_{k'3} - i_4\omega_a) \Bigg\}
\end{aligned}
$$

0954-4062/93 $3.00 + .05

$$+\sum_{n=1}^{n_0}\sum_{q=1}^{3}\left\{\sum_{i_3}\sum_{i_2}\sum_{i_4} G_{\mathrm{T}n}(i_3\,\omega_g) \times K'_{\mathrm{T}nq}(i_2\,\omega_{k'q})A_{\mathrm{T}nm}(i_4\,\omega_a) \times \delta(\omega - i_3\,\omega_g - i_2\,\omega_{k'q} - i_4\,\omega_a)\right\}\Bigg] \times H_m(\omega) + W_m(\omega) \quad (1)$$

where δ and δ_{T} are the Dirac and the Kronecker delta functions respectively; the sub-index n indicates the nth roller and n_0 is the roller number; the super-index s means that the vibration is induced by the surface irregularities; H_m is the Fourier transformation of $\exp(-\alpha_m t)\cos(\omega_m t)$ (bearing structure properties) and W_m describes the frequency characteristics of noises; $Y_{\mathrm{T}np}$ and $G_{\mathrm{T}n}$ are the Fourier transforms of surface irregularities of races and rollers respectively; $K'_{\mathrm{T}nq}$ and $A_{\mathrm{T}nm}$ are the Fourier transforms of the equivalent stiffness and transmission path; ω_a is the frequency of the transmission path, ω_{yp} and $\omega_{k'q}$ are the frequencies of the race profile and equivalent stiffness relative to the cage respectively and ω_g is the roller defect frequency. The terms in the first and second braces describe the effects of geometric irregularities of races on vibrations. The effect of roller errors is indicated by the term in the third brace. The delta functions of equation (1) render the vibration spectra of undamaged bearings having peaks at frequencies

$$\omega = i_1\omega_{yp} + i_2\,\omega_{k'q} + i_4\,\omega_a \quad (2a)$$

or

$$\omega = i_3\,\omega_g + i_2\,\omega_{k'q} + i_4\,\omega_a \quad (2b)$$

If the noise term W_m is ignored, the vibration spectra will show an EFSD pattern (**4**, **5**). If the noise energy dominates, due to the uncertainty of spectrum estimation (**7**), the peaks may not appear and the EFSD pattern is vague.

The terms in the second and third braces of equation (1) are negligible, if the race waviness dominates the roller errors. The term in the second bace is negligible partly because of the random essence of k'_{n3} (the time domain function of $K'_{\mathrm{T}n3}$) (**4**). On the other hand, if the roller errors dominate, X^{s}_m is mainly determined by the term in the third brace. Because $\omega_{k'1} = \omega_a$ (**4**), the magnitude of the main peak (with frequency equal to the multiple of defect frequency) is primarily decided by

$$n_0\sum_{i_2}\sum_{i_4} Y_{\mathrm{T}1p}(jn_0\omega_{yp})K'_{\mathrm{T}11}(i_2\,\omega_a)A_{\mathrm{T}1m}(i_4\,\omega_a)$$

(if race errors dominate)

or

$$\sum_{n=1}^{n_0}\sum_{i_2}\sum_{i_4} G_{\mathrm{T}n}(j\omega_{\mathrm{roll}})K'_{\mathrm{T}n1}(i_2\,\omega_a)A_{\mathrm{T}nm}(i_4\,\omega_a)$$

(if roller errors dominate)

with j = integer and $i_2 + i_4 = 0$. The magnitude of a specific side band corresponding to the above main peak is dominated by

$$n_0\sum_{q=1}^{2}\sum_{i_2}\sum_{i_4} Y_{\mathrm{T}1p}(jn_0\omega_{yp})K'_{\mathrm{T}1q}(i_2\,\omega_{k'q})A_{\mathrm{T}1m}(i_4\,\omega_a)$$

or

$$\sum_{n=1}^{n_0}\sum_{q=1}^{3}\sum_{i_2}\sum_{i_4} G_{\mathrm{T}n}(j\omega_{\mathrm{roll}})K'_{\mathrm{T}nq}(i_2\,\omega_{k'q})A_{\mathrm{T}nm}(i_4\,\omega_a)$$

with $i_2\,\omega_{k'q} + i_4\,\omega_a$ = constant (whose value is equal to the frequency interval between the side band and main peak). From above, the relative magnitude between the side band and main peak can be approximately measured by the index

$$\eta = \frac{\sum_{q=1}\sum_{j_1}\sum_{j_2} K'_{\mathrm{T}nq}(j_1\omega_{k'q})A_{\mathrm{T}nm}(j_2\,\omega_a)}{\sum_{j_3}\sum_{j_4} K'_{\mathrm{T}n1}(j_3\,\omega_a)A_{\mathrm{T}nm}(j_4\,\omega_a)} \quad (3)$$

with $j_1\omega_{k'q} + j_2\,\omega_a$ = constant and $j_3 + j_4 = 0$. The index η is defined as the magnitude ratio between the side band and main peak.

If the value of η is large, the magnitude of the side band relative to that of its corresponding main peak is large. On the other hand, the main peak dominates the side bands when the value of η is much less than 1. It is noted that η is not directly related to the frequency characteristics of surface irregularities. Its value is determined by the location of measurement and the distribution of equivalent stiffness (or equivalently the loading distribution) along the circumference of the outer race. When examining the denominator and the numerator of η, it is found that the value of η is assumed to be small if

$$|K'_{\mathrm{T}nq}(0)| \gg |K'_{\mathrm{T}nq}(i_2\,\omega_{kq})| \quad (4a)$$

and for $i_2, i_4 \neq 0$

$$|A_{\mathrm{T}nm}(0)| \gg |A_{\mathrm{T}nm}(i_4\,\omega_a)| \quad (4b)$$

The above condition indicates that η is small when the d.c. components of $k'_{nq}(t)$ (the equivalent stiffness function of the nth roller) and $a_{nm}(t)$ (the transmission path function of the nth roller) are much larger than their low-frequency components (say with frequency less than half of the interval between two consecutive main peaks). It is shown in reference (**5**) that the frequency characteristic of k'_{nq} is similar to that of the oil-film stiffness between roller n and each race. The low-frequency characteristics of oil-film stiffness depend on the distribution of external loading and the size of surface waviness (especially the surface waviness of the outer race or the inner race). If the external loading distribution tends to be uniform and the surface waviness is small (as compared to the minimum film thickness), the ratio between the d.c. component and the low-frequency component of k'_{nq} is small. However, for most running conditions, the magnitude of the minimum film thickness has the same order (with a magnitude less than 1 μm) as that of surface waviness. Thus, for undamaged bearings, the d.c. value of k'_{nq} will not be significantly larger than its low-frequency component, whether the loading distribution is uniform or not.

The ratio between the d.c. component and the low-frequency component of a_{nm} mainly depends on the sensor location, the measurement direction and the structure characteristics. Since the location of roller n revolves as the shaft runs, a_{nm} is a time-varying function. If the sensor location and the measurement direction are arranged so that a_{nm} is not seriously affected by the change of roller position, a_{nm} tends to be a constant time function and $|A_{\mathrm{T}nm}(0)|$ is much larger than

$|A_{Tnm}(i_4\omega_a)|$. Otherwise, $|A_{Tnm}(0)|$ and $|A_{Tnm}(i_4\omega_a)|$ are comparable. However, due to the rectification effect, $|A_{Tnm}(0)|$ will be enhanced when examining the demodulated signal. Thus, $|A_{Tnm}(0)|$ has a good chance of significantly exceeding $|A_{Tnm}(i_4\omega_a)|$ when investigating the demodulated spectra.

The above discussion demonstrates that in most cases $|K'_{Tnq}(0)|$ is unlikely to be much larger than $|K'_{Tnq}(i_2\omega_{kq})|$, although $|A_{Tnm}(0)|$ may exceed $|A_{Tnm}(i_4\omega_a)|$. Hence, conditions (4a) and (4b) can not be simultaneously satisfied and η will not be a small value. As a result, for undamaged roller bearings, the size of the main peak will have the same order as that of its corresponding side bands.

3 MAGNITUDE CHARACTERISTICS OF VIBRATION SPECTRA FOR DAMAGED ROLLER BEARINGS

If a roller bearing has surface damage, the bearing vibrations can be assumed to be the sum of surface-induced vibration and damage-induced vibration (**4**). The damage-induced vibration comes from the periodic excitation of the pulse train $k''_n(t)d_n(t)$ (**2**), where k''_n describes the sensitivity of striking energy for the nth roller and is a function of the loading sustained by roller n and d_n depicts the dimension information of surface damage. If damage has occurred at the ith roller, d_n is a pulse train for $n = i$ and d_n is zero for $n \neq i$. For inner or outer race damage, d_n is also a pulse train and d_i is related to d_{i+1} by a transportation lag. Thus d_n and k''_n are periodic functions with periodicities related to damage location, bearing geometry, external loading and running speed (**1**) when the bearing runs at a constant speed. Similarly, the frequency characteristics of damage-induced vibration can be described by

$$X^{d}_{m}(\omega) = \left\{ \sum_{n=1}^{n_0} \sum_{q} \sum_{i_5} \sum_{i_6} \sum_{i_4} D_{Tn}(i_5\omega_d) \times K''_{Tnq}(i_6\omega_{k''q}) A_{Tnm}(i_4\omega_a) \times \delta(\omega - i_5\omega_d - i_6\omega_{k''q} - i_4\omega_a) \right\} H_m(\omega) \quad (5)$$

where the super-index d indicates the damage-induced vibration, D_{Tn} is the Fourier transform of d_n and K''_{Tnq} is the Fourier transform of the single-periodicity function of k''_n (**4**, **5**). Because the frequency nature of D_{Tn} or K''_{Tnq} is the same as that of Y_{Tnp} (or G_{Tn}) or K'_{Tnq}, the damaged-induced vibration spectra have peaks at the same frequencies as those of undamaged bearings.

From equation (5), the magnitude ratio between the side band and main peak due to surface damage can be written as

$$\eta = \frac{\sum_{q} \sum_{j_1} \sum_{j_2} K''_{Tnq}(j_1\omega_{k''q}) A_{Tnm}(j_2\omega_a)}{\sum_{j_3} \sum_{j_4} K''_{Tns}(j_3\omega_{k''s}) A_{Tnm}(j_4\omega_a)}$$

with $\omega_{k''s} = \omega_a$, $j_1\omega_{k'q} + j_2\omega_a =$ constant and $j_3 + j_4 = 0$. When K'_{Tnq} is substituted by K''_{Tnq} in condition (4a), the value of η is assumed to be small if conditions (4a) and (4b) are satisfied. The nature of the transmission path a_{nm} for a damaged bearing is the same as that for an undamaged bearing. When surface damage is on the outer race and the sensor is located at a fixed site, the transmission path a_{nm} is a constant and condition (4b) is always satisfied. If the sensors are so placed that the transmission path between the measurement and damage-induced impulse is little affected by the location change of the damage spot, the d.c. component of a_{nm} can be much larger than its low-frequency components. In examining the demodulated spectra, the condition (4b) also tends to be satisfied due to signal rectification. Thus, $|A_{Tnm}(0)|$ can be much larger than $|A_{Tnm}(i_4\omega_a)|$ if the sensor location is properly chosen.

The d.c. component of K''_{Tnq} will significantly exceed its low-frequency components if the external loading along the circumference of the outer race has a uniform distribution. As stated above, k''_n depends on the loading of roller n. If the external loading distribution is uniform, k''_n is a constant and condition (4a) is satisfied. On the other hand, if the bearing has inner race or roller damage and has sustained a large radial loading as compared to the axial loading, the d.c. value of k''_n will have the same order as its low-frequency components. Condition (4a) will then not necessarily be satisfied. When the bearing has outer race damage and is under stationary loading, the magnitudes of the main peaks are large and those of the side bands vanish. Consequently, for damage-induced vibration, η is small if the sensor is properly located and the external loading is uniform.

The above study shows that under uniform loading the magnitude information of the damage-induced EFSD pattern is assumed to be different from that of the surface-induced EFSD pattern. In the damage-induced EFSD pattern, the magnitudes of the main peaks are significantly large relative to those of the side bands. Conversely, in the surface-induced EFSD pattern, the magnitudes of the main peaks have the same order as those of the side bands. Thus, by examining the relative magnitudes between the main peaks and side bands, the vibration signatures between undamaged bearings and damaged ones are distinguishable.

In most cases, for a damaged bearing the measured vibrations will contain the signatures of the surface-induced vibration and the damage-induced vibration. Both types of vibrations will produce the EFSD pattern. For undamaged bearings, the EFSD pattern is enhanced by large surface irregularities, high running speed or large axial loading. The EFSD pattern for a damaged bearing is strengthened by large damage or high loading. If surface damage is small, the vibration energies induced by surface irregularities can not be ignored as compared to those induced by surface damage. Thus, the EFSD patterns due to surface irregularities and surface damage may be simultaneously detected in the vibration spectra. If surface damage is large, the damage-induced vibration will be dominant in the measured signal. The EFSD pattern due to surface damage may be the only signature observed. In most cases, the frequency bandwidth of bearing structure excited by the damage-induced impact is wider than that by the surface irregularities. Irrespective of the damage size, there exists a high-frequency band where the surface-induced vibration is negligible and the damage-induced vibration is dominant. Accordingly, if such a high-frequency band is examined, the damage-induced EFSD pattern will dominate the surface-

induced EFSD pattern such that only the first one is observed.

4 EXPERIMENTAL STUDY

To verify the above analytical study, the demodulated spectra of an undamaged tapered roller bearing (SKF type 32208) and three damaged bearings were examined. The description of the test rig can be found in reference (5). The electrical-discharge machining method was applied to produce artificial damage on the bearing surfaces. The damage sizes are shown in Table 1. The vibration signal was measured by mounting an accelerometer on the housing, which is close to the test bearing. The measured direction is radial to the shaft. Two frequency bands of vibration characteristics were investigated, from 4.8 to 6.4 kHz (designated as the low-frequency band) and from 12 to 15 kHz (designated as the high-frequency band). These bands are assumed to be the frequency bands of two modes of bearing assembly based on the experimental data. To study the wavelength characteristics of surface irregularities for an undamaged bearing, the surface profiles of components were measured by a roundness-measuring instrument. All of the tested bearings were run at 2000 r/min. At this speed, the surface profile with wavelength of 0.3 mm is equivalent to a sinusoidal function with a frequency of 10 kHz.

The wavelength spectra of a new bearing (after 3 hours of running) are plotted in Fig. 1. It shows that the roller errors dominate the race irregularities. Also, the spectra present a trend that the smaller the wavelength, the smaller the magnitude of surface profile. The demodulated spectra of vibrations at the low- and the high-frequency bands under axial preload are shown in Fig. 2. All of the peaks in the spectra are predicted by equation (2). The demodulated spectra indicate that there are obvious EFSD patterns with a roller message at both frequency bands. This is because the roller errors have dominant energy as compared to the race irregularities at the examined frequency bands. The measured magnitude ratios between the first main peak and its side bands are listed in Table 2. The results demonstrate that the magnitude of the main peak has the same order as that of its side bands.

Table 1 Damage sizes of defective bearings

Damaged type	Damage size (length × width × depth) mm
Roller	16 × 0.25 × 0.1
Inner race	14 × 0.15 × 0.1
Outer race	18.5 × 0.25 × 0.1

The demodulated spectra for the roller defect bearing under light and large axial preloads are shown in Fig. 3. All of the observed peaks can be predicted by equation (2). The measured magnitude ratios are listed in Table 3. It is shown that under light preload the magnitude of the main peak is significantly larger than that of its side bands at both the low- and the high-frequency bands. However, under a large preload, the energies of the side bands are relatively large at the low-frequency band. This is because under light preload the surface-induced message is negligible and only the damage-induced pattern is revealed. However, with a large preload, the surface-induced pattern is enhanced at the low-frequency band and both types of EFSD pattern are included in the low-frequency band. The above results also show that the magnitude information of the surface-induced EFSD pattern is different from that of the damage-induced one.

The demodulated spectra for the inner race and outer race defect bearings are shown in Figs 4 and 5 respectively. The measured magnitude ratios are listed in Tables 4 and 5. Similarly, under a light axial preload, the spectra only reveal the damage-induced EFSD pattern. However, under a large axial preload and at the low-frequency band, the surface-induced (from roller errors) and the damage-induced EFSD patterns all

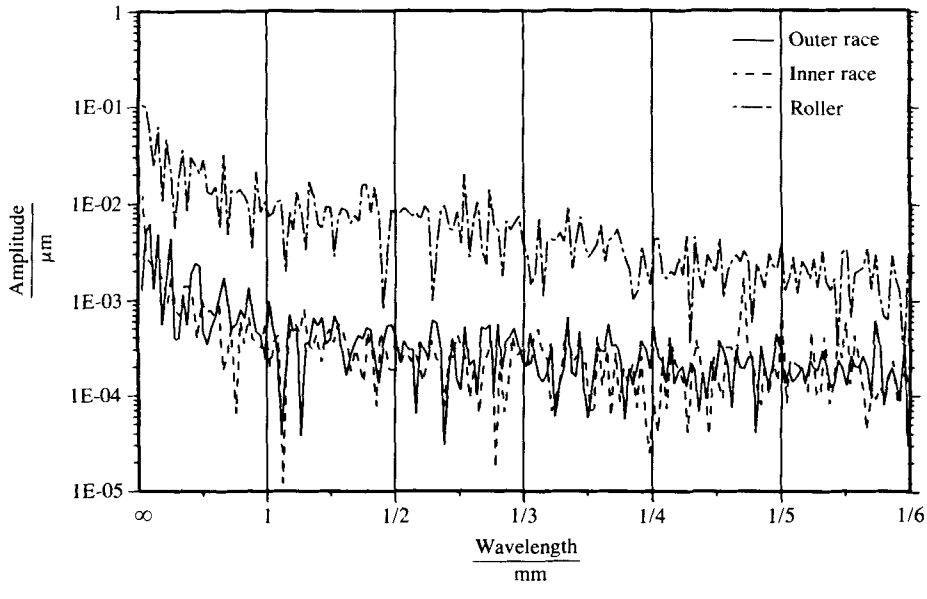

Fig. 1 Wavelength spectrum of bearing surface profiles

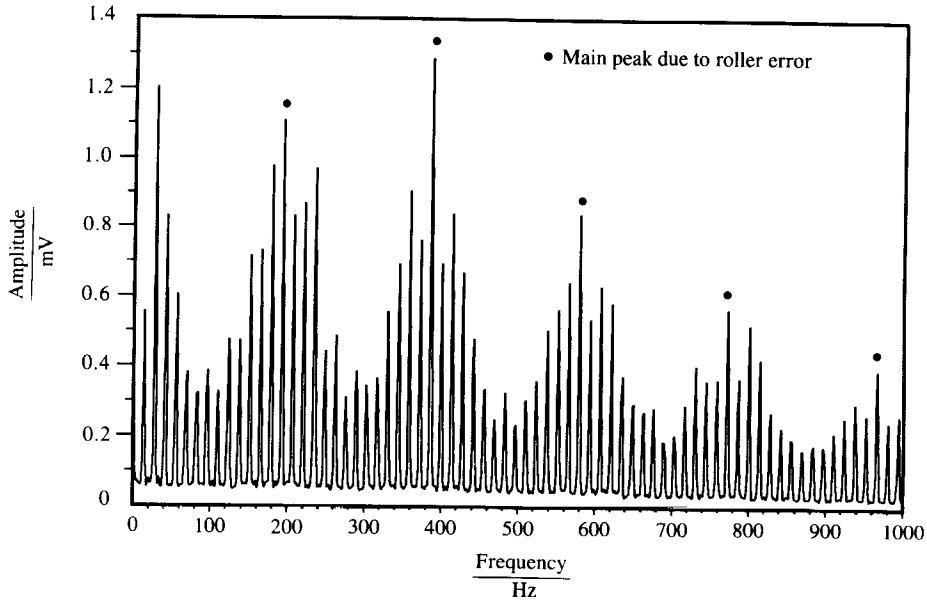

(a) At low-frequency band

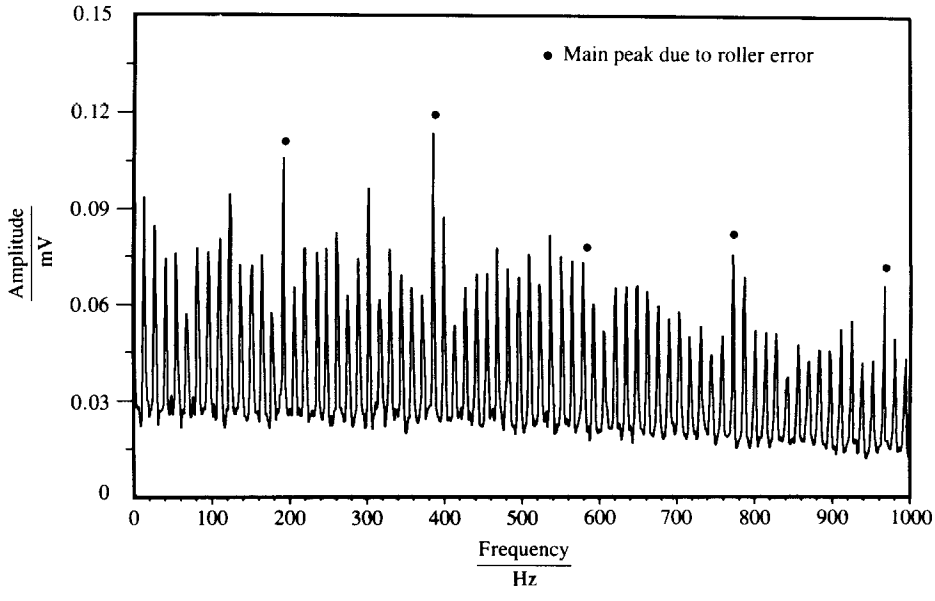

(b) At high-frequency band

Fig. 2 Demodulated spectra for normal bearing

appeared in the demodulated spectra. At the high-frequency band, the surface-induced EFSD pattern is not clear, even under a large preload. It is noted that when the damage size is further enlarged only the damage-induced EFSD pattern at both frequency bands exists, irrespective of the magnitude of the preload. If a radial loading is added to the roller defect bearing, the demodulated spectrum at the high-frequency band is shown in Fig. 6. The figure indicates that the side bands are enhanced under non-uniform loading. A similar

Table 2 The measured magnitude ratios between side bands and main peak for normal bearing

Main peak frequency Hz	Side band frequency Hz	Magnitude ratio under light preload at low-frequency band	Magnitude ratio under light preload at high-frequency band
193	137	0.4257	0.6841
	151	0.6453	0.6816
	165	0.6597	0.7115
	179	0.8822	0.5423
	207	0.7504	0.6199
	221	0.7836	0.7318
	235	0.8762	0.7199
	249	0.4002	0.7320

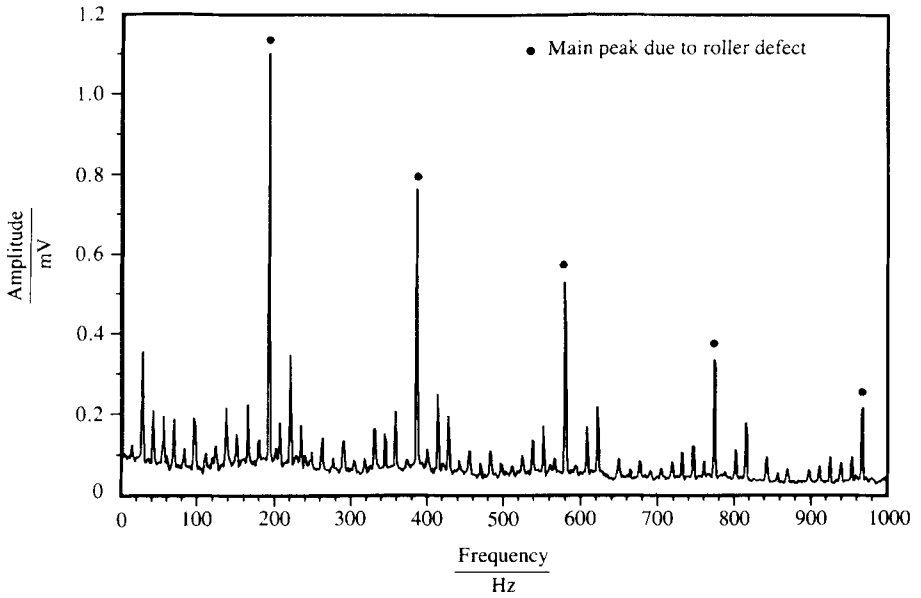

(a) Under light preload at low-frequency band

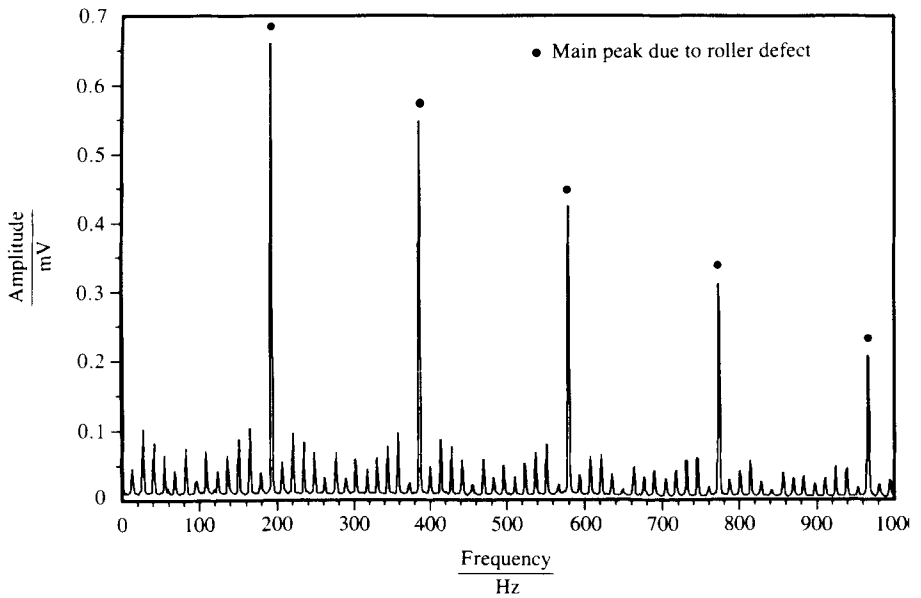

(b) Under light preload at high-frequency band

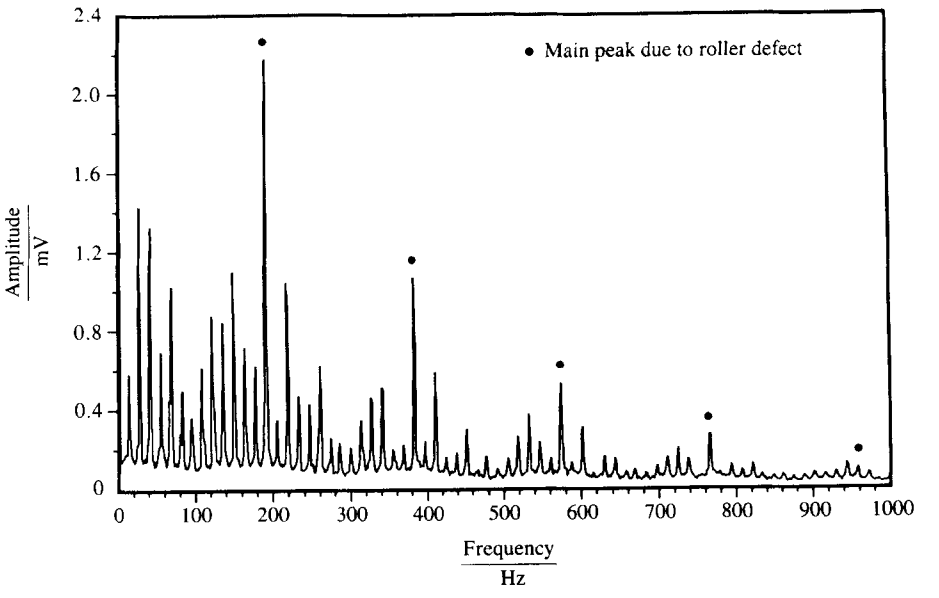

(c) Under large preload at low-frequency band

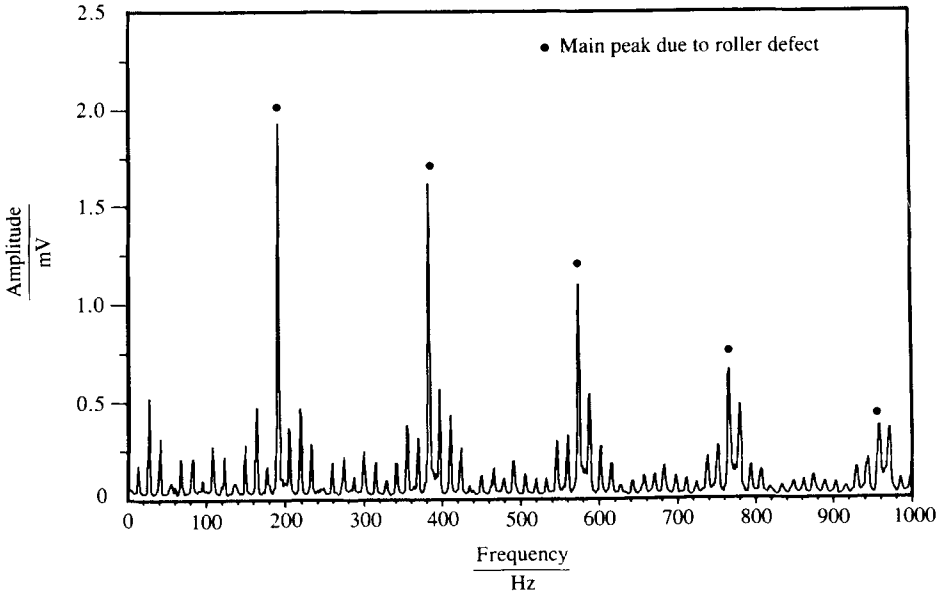

(d) Under large preload at high-frequency band

Fig. 3 Demodulated spectra for roller defect bearing

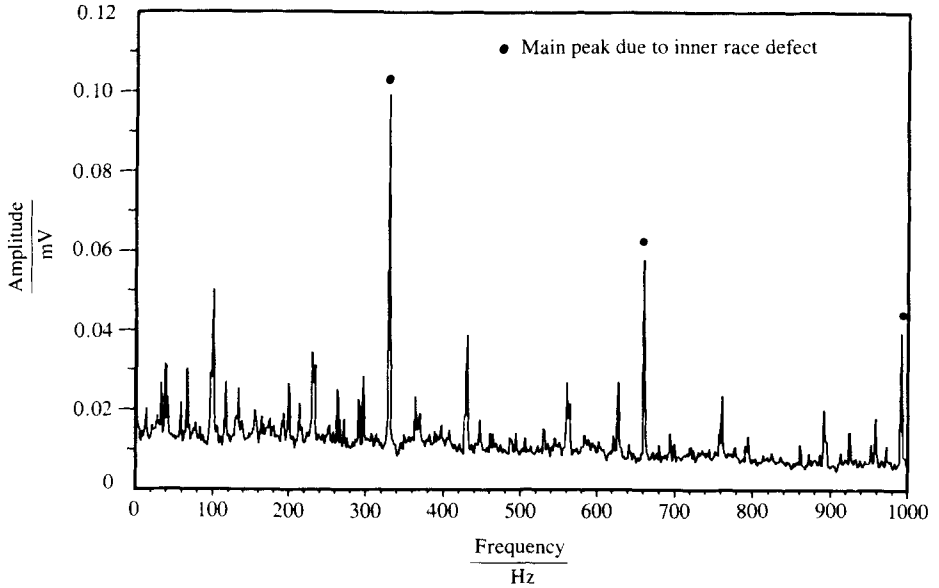

(a) Under light preload at low-frequency band

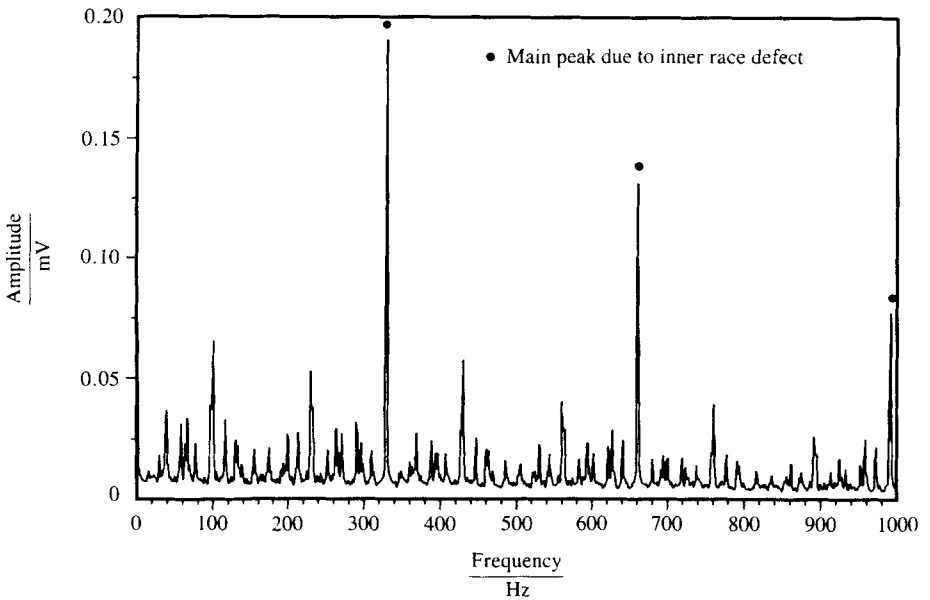

(b) Under light preload at high-frequency band

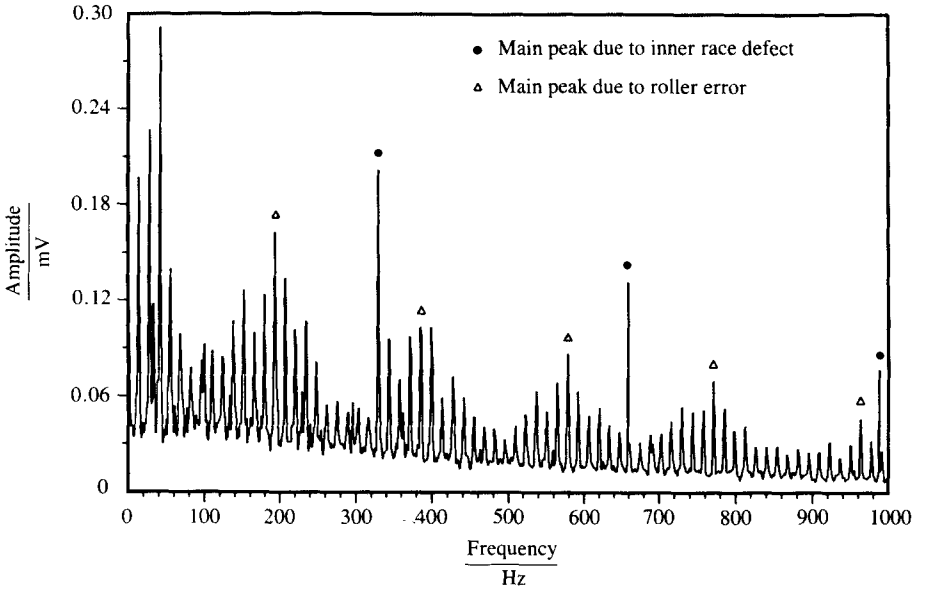

(c) Under large preload at low-frequency band

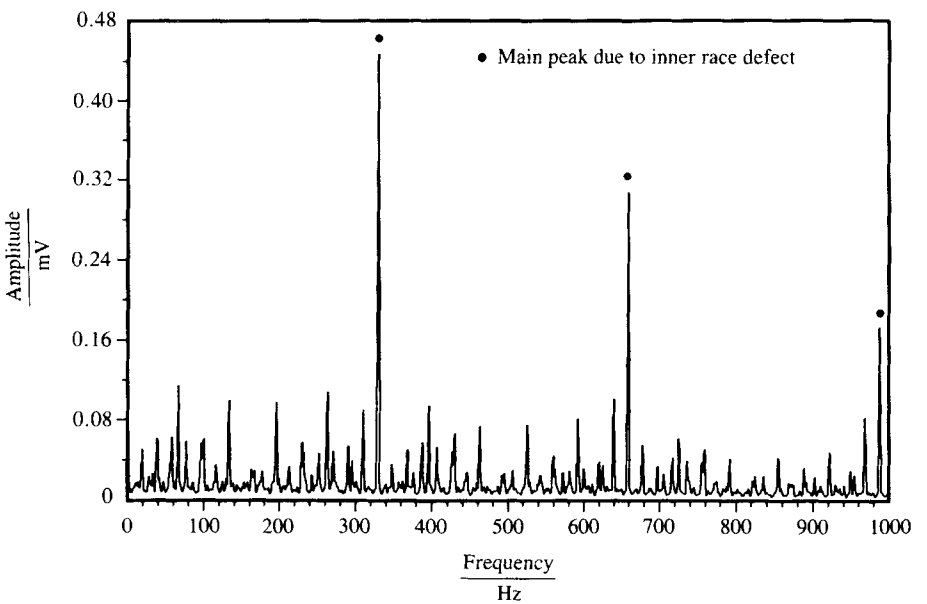

(d) Under large preload at high-frequency band

Fig. 4 Demodulated spectra for inner race defect bearing

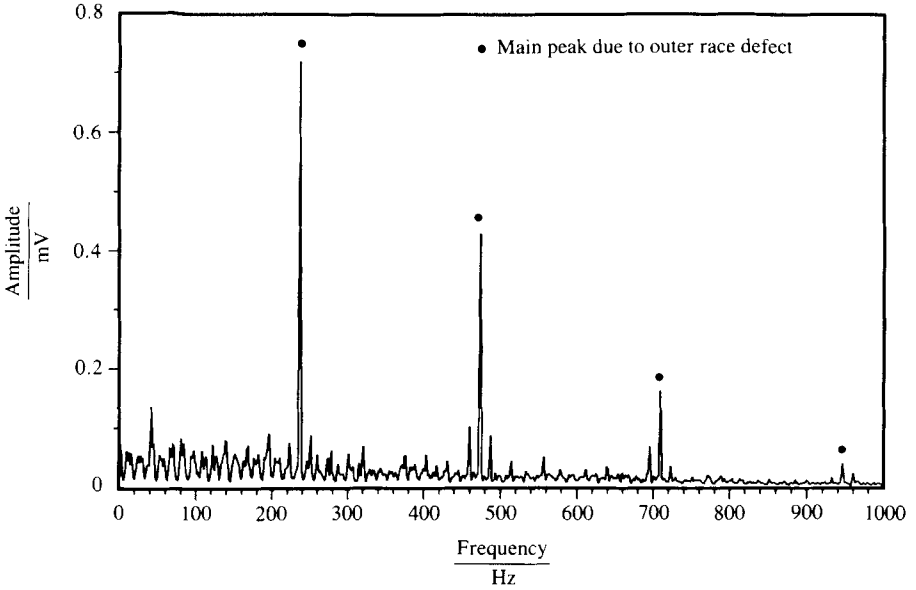

(a) Under light preload at low-frequency band

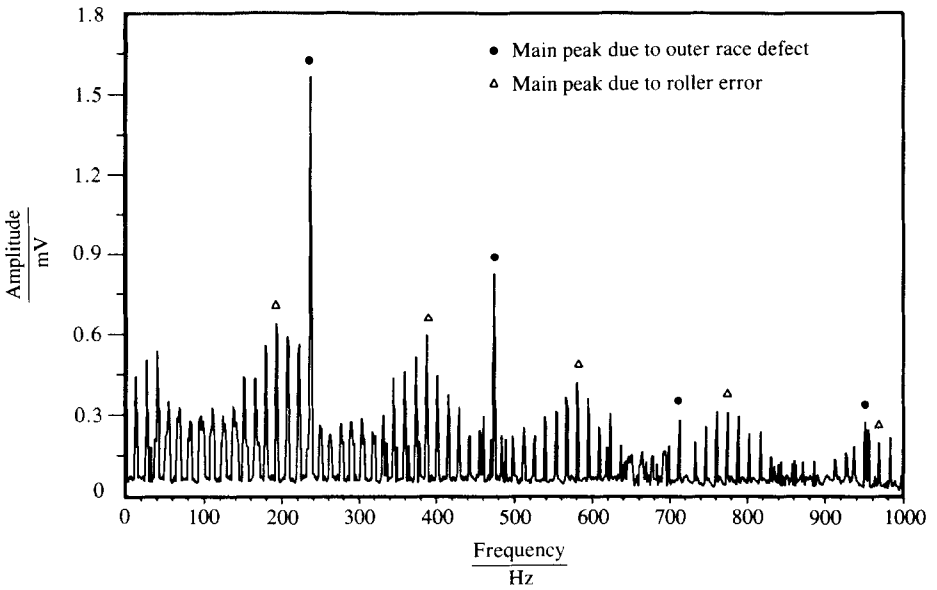

(c) Under large preload at low-frequency band

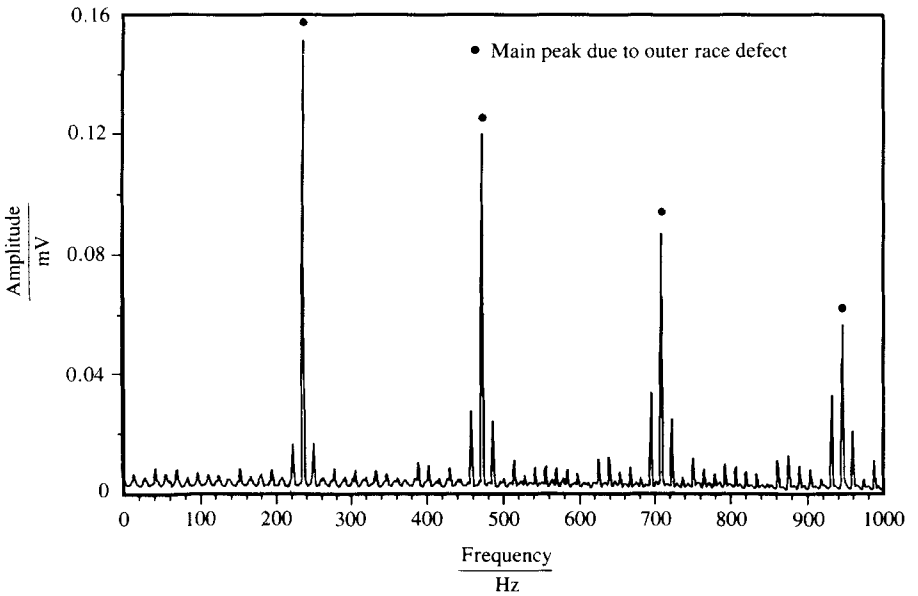

(b) Under light preload at high-frequency band

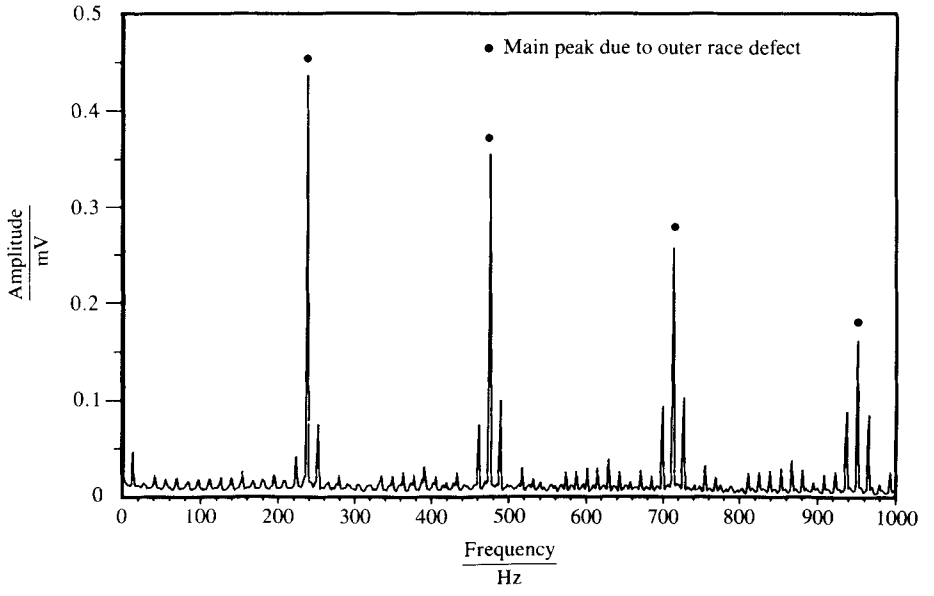

(d) Under large preload at high-frequency band

Fig. 5 Demodulated spectra for outer race defect bearing

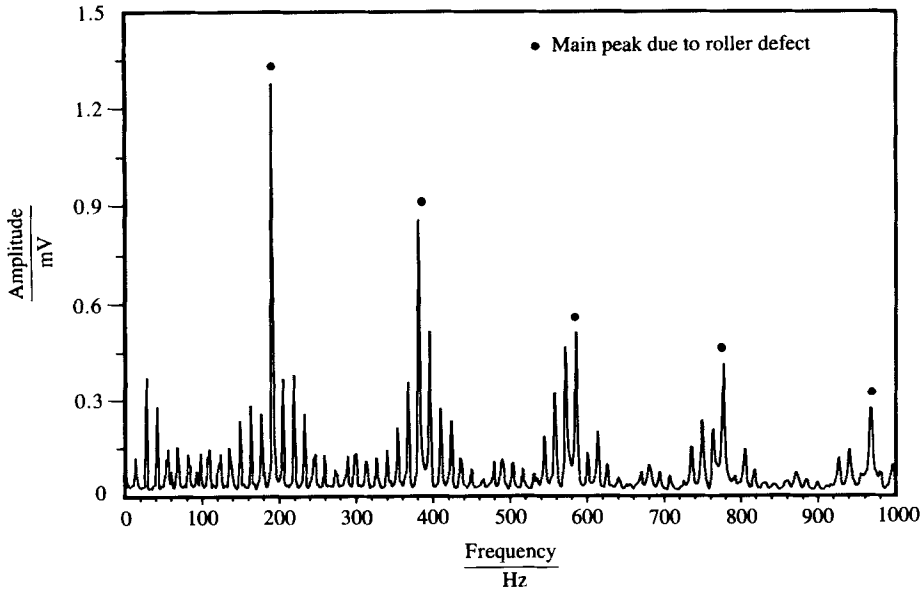

Fig. 6 Demodulated spectrum at high-frequency band for roller defect bearing under radial loading

result may be obtained when a radial loading is added to the inner race defect bearing. The radial loading has little effect on the side band energy for the outer race defect bearing because the transmission path between damage and measurement is fixed.

The above results clearly demonstrate that the magnitude information of the damage-induced EFSD patterns is different from that of the surface-induced EFSD patterns under uniform loading. In many running conditions, both types of EFSD patterns may appear in the low-frequency band. However, the damaged-induced EFSD pattern is dominant in a high-frequency band. When a non-uniform loading is added, the magnitudes of side bands may be enhanced for the inner race defect or roller defect bearings, which will increase the difficulty of distinguishing the damage-induced pattern from the surface-induced one.

5 CONCLUSIONS

This study has shown that the magnitude information of the damage-induced EFSD patterns is different from that of the surface-induced EFSD patterns under uniform loading. The magnitude of the main peak is significantly larger than that of the side bands for the

Table 3 The measured magnitude ratios between side bands and main peak for roller defect bearing

Main peak frequency / Hz	Side band frequency / Hz	Magnitude ratio under light preload at low-frequency band	Magnitude ratio under light preload at high-frequency band	Magnitude ratio under large preload at low-frequency band	Magnitude ratio under large preload at high-frequency band
193	137	0.195	0.0989	0.3881	0.0446
	151	0.136	0.1344	0.5049	0.1453
	165	0.2031	0.1581	0.3294	0.2452
	179	0.1243	0.0621	0.2858	0.0883
	207	0.1629	0.0832	0.1618	0.1899
	221	0.3152	0.1467	0.4801	0.2434
	235	0.1572	0.1262	0.2156	0.1485
	249	0.0944	0.1037	0.1981	0.0331

Table 4 The measured magnitude ratios between side bands and main peak for inner race defect bearing

Main peak frequency / Hz	Side band frequency / Hz	Magnitude ratio under light preload at low-frequency band	Magnitude ratio under light preload at high-frequency band	Magnitude ratio under large preload at low-frequency band	Magnitude ratio under large preload at high-frequency band
330	198	0.2681	0.1403	0.8078	0.1821
	231	0.3475	0.2762	0.3095	0.1075
	264	0.2544	0.1533	0.2698	0.2020
	297	0.2863	0.1222	0.2753	0.0743
	363	0.2353	0.1425	0.2441	0.0924
	396	0.1641	0.1003	0.5110	0.1747
	429	0.3903	0.3008	0.3582	0.1237
	462	0.1422	0.1043	0.2023	0.1381

Table 5 The measured magnitude ratios between side bands and main peak for outer race defect bearing

Main peak frequency Hz	Side band frequency Hz	Magnitude ratio under light preload at low-frequency band	Magnitude ratio under light preload at high-frequency band	Magnitude ratio under large preload at low-frequency band	Magnitude ratio under large preload at high-frequency band
236	180	0.0801	0.0425	0.3568	0.0412
	194	0.1260	0.0515	0.4077	0.0512
	208	0.0701	0.0348	0.3773	0.0391
	222	0.1065	0.1078	0.3592	0.0957
	250	0.1218	0.1098	0.1617	0.1732
	264	0.0408	0.0322	0.1459	0.0363
	278	0.0865	0.0556	0.1695	0.0517
	292	0.0328	0.0368	0.1765	0.0310

damage-induced EFSD pattern. On the other hand, the magnitude of the main peak has the same order as that of its side bands for surface-induced EFSD patterns. In many running conditions, for a damaged roller bearing, both types of EFSD patterns may appear in a low-frequency band. However, the damaged-induced pattern is dominant in a high-frequency band. Hence, it is possible to distinguish a damaged roller bearing from undamaged ones by inspecting both the frequency information and the magnitude information of demodulated spectra at a high-frequency band. However, the study also indicates that the magnitudes of side bands may be enhanced due to non-uniform loading. Thus, to diagnose the bearing quality reliably, some other indices (such as statistic indices of time domain signals) and a decision system (such as an expert system) might be helpful.

REFERENCES

1 **Su, Y.-T.** and **Lin, S.-J.** On initial fault detection of tapered roller bearing: frequency domain analysis. *J. Sound Vibr.*, 1992, **155**(1), 75–84.

2 **McFadden, P. D.** and **Smith, J. D.** Model for the vibration produced by a single point defect in a rolling element bearing. *J. Sound Vibr.*, 1984, **96**, 69–92.

3 **McFadden, P. D.** and **Smith, J. D.** Vibration monitoring of rolling element bearings by the high-frequency resonance technique—a review. *Int. J. Tribology*, 1984, **17**, 3–10.

4 **Su, Y.-T., Lin, M.-H.** and **Lee, M.-S.** The effects of surface irregularities on roller bearing vibrations. *J. Sound Vibr.*, 1993, **162** (to appear).

5 **Su, Y.-T., Sheen, Y.-T.** and **Lin, M.-H.** Signature analysis of roller bearing vibrations: lubrication effects. *Proc. Instn Mech. Engrs, Part C*, 1992, **206**(C3), 193–202.

6 **Sunnersjö, C. S.** Rolling bearing vibrations—the effects of geometrical imperfections and wear. *J. Sound Vibr.*, 1985, **98**, 445–474.

7 **Jenkins, G. M.** and **Watts, D. G.** *Spectral analysis and its applications*, 1969 (Holden-Day Inc., San Francisco, Calif.).